ResearchGate

See discussions, stats, and author profiles for this publication at: https://www.researchgate.net/publication/327551472

# Random Forest Classification using Sentinel-1 and Sentinel-2 series for vegetation monitoring in the Pays de Brest (France)

**Conference Paper** · September 2018

DOI: 10.1117/12.2325546

CITATIONS
18

READS
4,006

**3 authors:**

Simona Niculescu
Université de Bretagne Occidentale
**71** PUBLICATIONS **211** CITATIONS

SEE PROFILE

Antoine Billey
Université de Bretagne Occidentale
**10** PUBLICATIONS **28** CITATIONS

SEE PROFILE

Halima Talab Ou Ali
**8** PUBLICATIONS **33** CITATIONS

SEE PROFILE

**Some of the authors of this publication are also working on these related projects:**

Project

Nouvelles données satellites. Quel intérêt pour les Collectivités Locales ? Application aux changements de l'occupation du littoral du Pays de Brest. View project

Project

Remote Sensing and Vegetation Monitoring in Pays de Brest (France) View project

All content following this page was uploaded by Simona Niculescu on 16 October 2018.

The user has requested enhancement of the downloaded file.

PROCEEDINGS OF SPIE

SPIEDigitalLibrary.org/conference-proceedings-of-spie

# Random forest classification using Sentinel-1 and Sentinel-2 series for vegetation monitoring in the Pays de Brest (France)

Simona Niculescu, Antoine Billey, Halima Talab-Ou-Ali

Simona Niculescu, Antoine Billey, Halima Talab-Ou-Ali, "Random forest classification using Sentinel-1 and Sentinel-2 series for vegetation monitoring in the Pays de Brest (France)," Proc. SPIE 10783, Remote Sensing for Agriculture, Ecosystems, and Hydrology XX, 1078305 (9 October 2018); doi: 10.1117/12.2325546

SPIE.

Event: SPIE Remote Sensing, 2018, Berlin, Germany

Downloaded From: https://www.spiedigitallibrary.org/conference-proceedings-of-spie on 10/15/2018 Terms of Use: https://www.spiedigitallibrary.org/terms-of-use

# Random Forest Classification using Sentinel-1 and Sentinel-2 series for vegetation monitoring in the Pays de Brest (France)

Simona NICULESCU[1], Antoine BILLEY[2], Halima TALAB-OU-ALI[3]

[1, 2, 3] Université de Bretagne Occidentale, CNRS, LETG Brest UMR 6554
CNRS, France – simona.niculescu@univ-brest.fr

## ABSTRACT

Nowadays, optical and radar remote sensing data are increasingly used for land-cover/vegetation mapping and monitoring. Their technical capabilities and tools are improving all the time and provide more accurate results. By the recent arrival of the Sentinel-1 and Sentinel-2 series, available free, processing and methods of analysis must be increased more and more in the field of cartography. This paper aims to present vegetation mapping method in the Pays de Brest area by using a time series stacking of Sentinel-1, Sentinel-2 and SPOT-6 satellites data using the algorithm Random Forest supervised classification. The types of vegetation mapping in first time are those belonging to the major vegetation types, but especially those that can be observed on the processed images that are the Sentinel-1, Sentinel-2 series and SPOT-6. The types of classes considered for this study are: no vegetation, forest and undergrowth, moors and lawns, summer crops, winter crops, grassland and water. Several time series stacking has been made on that series containing 140 images radar representing different dates (2017) and the best combination method is to use both the two polarizations VV and VH to the calculation of the matrix of confusion. On the other hand, combinations of SAR images with different vegetation indices (NDVI, NDWI, S2rep, IRECI) calculated from the Images Sentinel-2 have been made. The series of times series stacking ends with combinations between SPOT-6 and Sentinel-1. The times series stacking Sentinel-1, Sentinel-2 and SPOT-6 are satisfactory, with an overall accuracy that reaches 93%. Such precision is very good for data that are available free.

**Keywords:** Random Forest, multi-temporal Sentinel-1, Sentinel-2 and SPOT-6, times series stacking, vegetation monitoring, Pays de Brest.

## 1- INTRODUCTION

As part of the European Copernicus program but also of national devices (Equipex GEOSUD, THEIA Cluster) the satellite data are becoming more and more easily accessible, at the level of the scientific community, companies or the general public. At the same time, the massive opening up of digital data in different forms (spatialized or not) and relating to different domains and their relationship with satellite data, opens up new avenues for research and applications. In the domain of the monitoring of vegetation in coastal zones, the arrival of new satellites such as the Sentinel-1 and 2 open up new prospects for research and applications.

Remote sensing is the most significant technology for effective vegetation mapping at large scales, bringing numerous advantages such as cost-effectiveness and repeatability of observations (Chilar, 2000; Kuemmerle et *al*., 2013). Vegetation bio-geophysical variable extraction, quantitatively retrieved and spatio-temporally explicit, is required in a variety of ecological and agricultural applications. Earth observation remote sensing focuses on the visible, infrared or microwaves regions and, based on that, two main classifications are done: optical and SAR (Synthetic Aperture RADAR) remote sensing. Radar and optical remote sensing data deliver complementary information, hence land cover classification tasks can take advantage of the fusion of both data types leading generally to increase mapping accuracy. Accurate vegetation

Remote Sensing for Agriculture, Ecosystems, and Hydrology XX, edited by Christopher M. U. Neale, Antonino Maltese,
Proc. of SPIE Vol. 10783, 1078305 · © 2018 SPIE · CCC code: 0277-786X/18/$18 · doi: 10.1117/12.2325546



Downloaded From: https://www.spiedigitallibrary.org/conference-proceedings-of-spie on 10/15/2018
Terms of Use: https://www.spiedigitallibrary.org/terms-of-use

mapping is essential for monitoring crop and sustainable agricultural practice. The processing requirements for such large data streams involve processing techniques enabling the spatio-temporally explicit quantification of vegetation properties. Typically retrieval must be accurate, robust and fast. The constellation Sentinel provide high operational ability, long-term continuity, superior calibration of sensors and a variety of sensing methods and products for the scientific community. Sentinel data distribution is supported by the key advantage of a full free and open access policy for the majority of the products.

In this research we explored the integrated use of the recently launched Sentinel-1A, Sentinel-2 A and SPOT-6 satellites for synergistic vegetation mapping exploiting radar and optical data, for a case study in Pays de Brest (France). Frequent revisit time is a major advantage over previous radar missions, especially for the mapping and analysis of phonological dynamics in vegetation and agricultural land covers, together with the dual polarization capability and rapid product delivery (Torres et al., 2012). Sentinel-2 (equipped with a multi-spectral instrument, MSI) sensor, launched on 23 June 2015 by the European Space Agency (ESA), provides a significant improvement in spectral coverage, spatial resolution, and temporal frequency over the current generation of Landsat sensors. For vegetation mapping Sentinel-2 is especially relevant for the presence of two new bands in the red edge spectrum, at 705 and 740 nm. Optical remote sensing uses the sun as an external source of irradiance and measures the reflected radiation from a surface in the visible and infrared part of the electromagnetic spectrum. In the visible part, green plants reflect radiation inversely related to the amount of radiation absorbed by their photosynthetic and accessory pigments. For example, the chlorophyll pigment absorbs most part of the radiation in the visible spectrum from 400 nm to 700 nm, especially at 430 nm (blue) and 660 nm (red) and leads to low reflectance in these bands (Chappelle, Kim, & McMurtrey, 1992). Contrarily, plant reflectance is high in the near infrared (NIR) region (700-1300 nm) as result of leaf inter-cellular structure, canopy density, and canopy structure effects (Mulla, 2013).

Unlike optical, SAR satellites use their own source of radiation. The microwave electromagnetic radiation used depends on the applications of each mission. In recent decades, SAR imagery has been shown to be advantageous for the estimation of vegetation-covered surfaces. SAR data are complementary to optical sensors, as their measurements mostly relate to the physical structure of the vegetation which is only partly described by the optical signal. By using active microwave radiation, SAR satellites can take advantage of its characteristics: penetration of waves in the ground (few centimetres), weather independence, and day-and-night imaging capability. Once the radiation is backscattered by a target, the sensor captures its strength and phase. The resulting value is directly linked with the wavelength, roughness, geometry, and material contents of the target.

The synergistic use of SAR and optical remote sensing was applied in several studies for describing vegetation in diverse ecosystems, for example, forests (Montesano et al. 2013; Reiche et al. 2015), wetlands (Rodrigues and Souza-Filho 2011; Hong et al. 2015; Niculescu et al., 2016, 2017), agricultural areas (Hill et al. 2005; Peters et al. 2011; Forkuor et al., 2014; Esch et al., 2014; Schuster et al., 2015; Bargiel, 2017), upland vegetation types (Barrett et al. 2016) and also to differentiate broad land cover classes (Ullmann et al. 2014).

In recent years, several algorithms developed for machine learning have been adopted for remote sensing applications. These include support vector machine, neural networks, and Random Forest. In opposition to parametric classifiers, a machine learning approach does not start with a data model but instead learns the relationship between the training and the response dataset (Breiman, 2001). Over the last decades, the Random Forest algorithm has received increasing attention due to good classification results and the speed of processing (Du, Samat, Waske, Liu, & Li, 2015; Rodriguez-Galiano, Ghimire, Rogan, Chica-Olmo, & Rigol-Sanchez, 2012; Belgiu § Dragut,2016).

## 2- STUDY SITE

The study site is the coastal areas in the Pays du Brest. The definition of the coastline is multiple, there is no strict definition. A definition which could be taken into consideration in this study is the definition of the region of Bretagne: "More than a simple line, the coastal zone should be viewed as a variable-geometry space whose limits on land and at sea are defined on the basis of the issue or the problem posed and responses" (Region of Brittany, 2007). Thus, it is considered for the



Downloaded From: https://www.spiedigitallibrary.org/conference-proceedings-of-spie on 10/15/2018
Terms of Use: https://www.spiedigitallibrary.org/terms-of-use

study that the whole country of Brest (including no point is located more than 20 km of the Sea) is in the coastal zone and will be processed in its globality.

The country of Brest is the association of an association of communes located north-west of Finistère in France (29) (figure 1). The country is affected by the presence of the sea, with its 370 km of coastal linear. The issues related to the environment are considerable, indeed the territory includes natural environments of quality and a high biodiversity. Nevertheless, these spaces are subjected to various pressures (densification of the urbanization in the littoral zone, a rise of sea level, pollution, invasive species ...) that make them vulnerable. These arguments are pushing the communities in favor of the establishment of a good management of their territories. It is as well the Natural Park Regional Armorique and the natural marine park the Iroise integrates in the Pays du Brest.

Figure 1: Geographical location of the country of Brest and the spatial distribution of its communes.

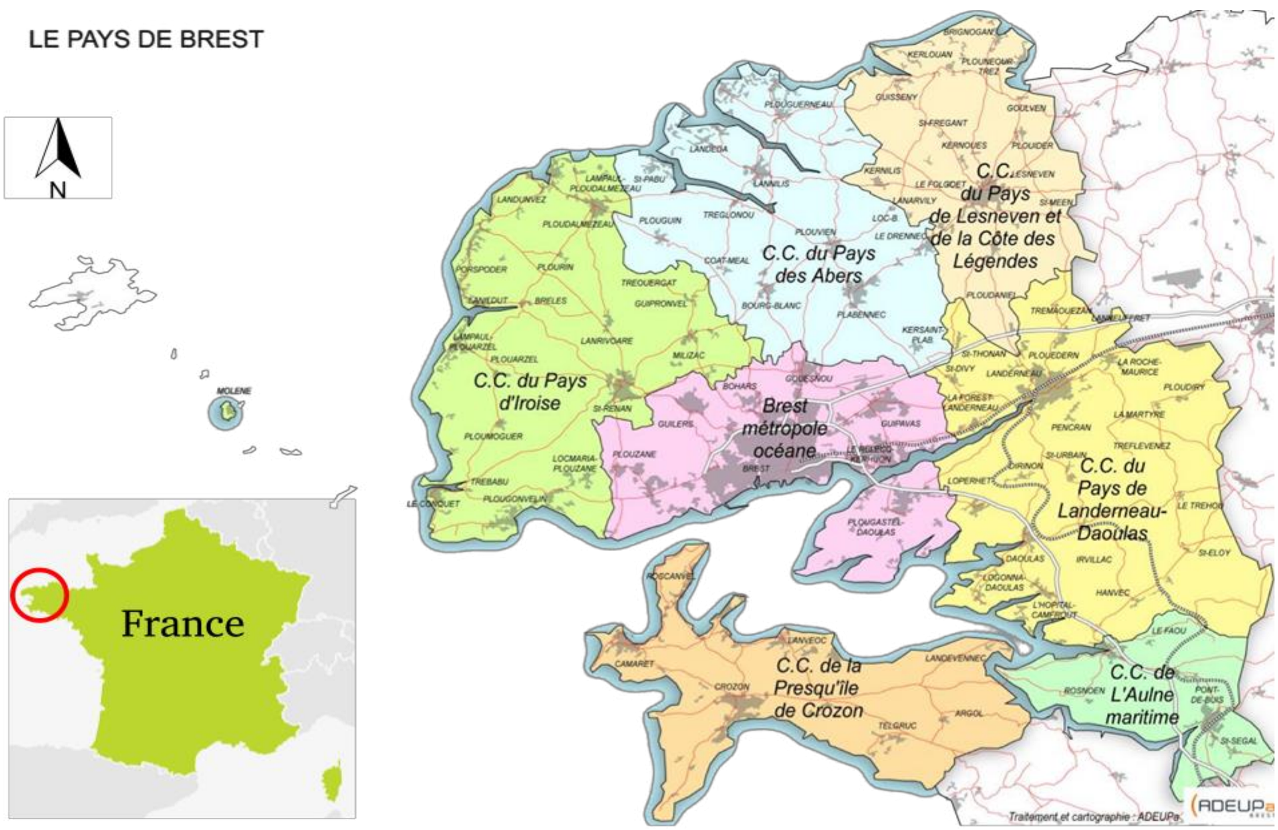


For the feasibility of processing and analysis of images, the territory of the country of Brest has been divided into 5 zones (Figure 2).



Downloaded From: https://www.spiedigitallibrary.org/conference-proceedings-of-spie on 10/15/2018
Terms of Use: https://www.spiedigitallibrary.org/terms-of-use

Figure 2: The division of the territory of the Pays de Brest in 5 zones

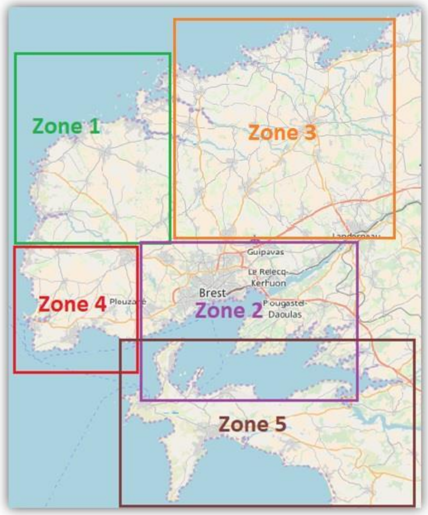


## 3- DATA SET

The satellite data processed for our study are from satellites Sentinel-1, Sentinel-2 and SPOT 6/7. All the satellite data were recorded during the year 2017.

The SPOT program (Satellites for the observation of the Earth) is the first European program dedicated to the observation of the earth. This program (1977), has been developed by the CNES (French National Center for Space Studies). The generation of satellites SPOT 6 and SPOT 7 (respectively launched in September 2012 and June 2014) takes over from the generation Spot 5 which its commercial service ended in 2015. Spot 6 and 7 are two satellites of the same satellites, with a sun-synchronous orbit and an orbital cycle of 26 days. The acquired images are simultaneously on 5 strips on scan swath of 60 km. In this study, Spot-6 satellite images with the resolution of 6 m were used (Table 1). Selected images corresponded to the inventory in terms of timing with suitable resolution. We used three images SPOT-6: the 16 June 2017, the 4 July 2017 and the 27 August 2017.

Table 1: Spatial resolution and Spectral resolution of SPOT-6/7

| Bandes | B1 Blue | B2 Green | B3 Red | B4 Infrared | B5 panchromatic |
|---|---|---|---|---|---|
| Spectrale resolution (nm) | 450-520 | 530-590 | 625-695 | 760 - 890 | 450-745 |
| Spatiale resolution (m) | 6 | 6 | 6 | 6 | 1,5 |

Launched in April 2014 for Sentinel-1A and in April 2016 for Sentinel-1B, these satellites operate with a synthetic aperture radar (SAR for Synthetic Aperture Radar). The Sentinel-1 data receives and transmits the waves with a frequency of 5.405 GHz, corresponding to a wavelength of approximately 5.6 cm (C-Band). The images are available in parallel polarization VV and cross polarization VH. With an orbit almost Polar and a temporal resolution of 12 days, these satellites allow to fly over the same area every 6 days, Sentinel-1 has therefore a fine temporal resolution. Interferometric Wide Swath (IW) allows to take measurements on scan swath of 250 km with a resolution of 5m on 20m. In addition three sub scan swath is possible thanks to the technique of the "Field Observation with Progressive Scan SAR" (TOPSAR), resulting in a superior image quality. 167 radar images in this format have been used for this study (Table 2).



Downloaded From: https://www.spiedigitallibrary.org/conference-proceedings-of-spie on 10/15/2018
Terms of Use: https://www.spiedigitallibrary.org/terms-of-use

Table 2: Sentinel-1 images available

| Data Sentinel-1 | | | | | |
|---|---|---|---|---|---|
| Orbit | Type of orbit | Angle of incidence | Polarization | Acquisition mode | Number of images |
| 1 | Ascending | 42° | VV/VH | IW | 52 |
| 52 | Descending | 33° | | | 31 |
| 103 | Ascending | 33° | | | 30 |
| 154 | Descending | 42° | | | 37 |

Launched in June 2015 for Sentinel 2A and in March 2017 for Sentinel-2B, these satellites are equipped with the optical instrument MSI (Multi-Spectral instrument), which covers 13 spectral bands from the visible through infrared. The Sentinel-2 mission is the continuation of programs Landsat and SPOT. These two satellites are able to provide images with a width at the ground of 290 km, and a periodicity of 5 days. Acquisitions are carried out according to three resolutions in function of the spectral band: 10, 20 and 60m (Table 3).

Table 3: Spatial and spectral resolutions of the Sentinel-2 satellite

| Band | B1 | B2 | B3 | B4 | B5 | B6 | B7 | B8 | B8a | B9 | B10 | B11 | B12 |
|---|---|---|---|---|---|---|---|---|---|---|---|---|---|
| Center λ (nm) | 443 | 490 | 560 | 665 | 705 | 740 | 783 | 842 | 865 | 945 | 1375 | 1610 | 2190 |
| Width λ (nm) | 20 | 65 | 35 | 30 | 15 | 15 | 20 | 115 | 20 | 20 | 30 | 90 | 180 |
| Spatial resolution (m) | 60 | 10 | 10 | 10 | 20 | 20 | 20 | 10 | 20 | 60 | 60 | 20 | 20 |

Several levels of correction are available during the download of images. The main levels available for our area of study as the level 1C and 2A. An image 1C has been ortho-rectified while an image 2A has in addition suffered an atmospheric correction. 10 optical images have been selected for our study described in the following table (Table 4).

Table 4: Sentinel-2 images available

| Data Sentinel-2 | | | | | | |
|---|---|---|---|---|---|---|
| Date of acquisition | 25/01/17 | 14/02/17 | 16/03/17 | 04/05/17 | 05/25/17 | 06/14/17 |
| Level of correction | 1C | 1C | 1C | 1C | 2A | 2A |



Downloaded From: https://www.spiedigitallibrary.org/conference-proceedings-of-spie on 10/15/2018
Terms of Use: https://www.spiedigitallibrary.org/terms-of-use

| Date of acquisition | 07/04/17 | 08/18/17 | 09/22/17 | 11/06/17 | 12/01/17 | 12/16/17 |
|---|---|---|---|---|---|---|
| Level of correction | 2A | 1C | 2A | 1C | 2A | 1C |

In this study we have also used other types of data (Table 5). These data have been integrated to the classification or which have resulted in a better knowledge of the area of study.

Table 5: Other data

| Data | Source | Scale of documents | Observations | Format |
|---|---|---|---|---|
| Land cover map of France 2016 | Cesbio | / | This map is available in vector and raster format. It is the result of the classification based on the data of the Sentinel-2 and Landsat ranging from end 2016 to end 2017. 17 classes that have been mapped on the whole France with a resolution of 10m. | Raster |
| Parcel Register Chart 2016 Edition | Administration | 1/5 000 | The parcel register graph is a geographic database to be used as reference for the statement of the aid of the common agricultural policy (PAC) data.gouv.fr | Vector |
| Corinne Land Cover 2012 | Administration | 1/25 000 | Land cover European database | Vector |
| BD_Topo | IGN | 1/5 000 | BD_ built, BD_Veget et BD_road | Vector |
| BD_Ortho | IGN | 0.50m | Mosaic of ortho-photos rectified in the Projection LAMBERT-93. These photos are in very high resolution and allow a good visualization of the field. They were of 2015. | Raster |

## 4- METHODOLOGY

The methodology of this article is composed of two major parties. A part concerning the classifications pixel by pixel of images Sentinel-1 and Sentinel-2 and a part on the classification of SPOT images-6. In the two parts the time series stacking of the results are carried out. On the one hand between the images Sentinel-1 and Sentinel-2 and the results of the various indices of vegetation from the optical images, and on the other hand, between the results of SPOT images and images Sentinel-1 (Figure 3). The algorithm chosen for the supervised classification is the Random Forest.



Downloaded From: https://www.spiedigitallibrary.org/conference-proceedings-of-spie on 10/15/2018
Terms of Use: https://www.spiedigitallibrary.org/terms-of-use

Figure 3: Pre-processing and Processing chain

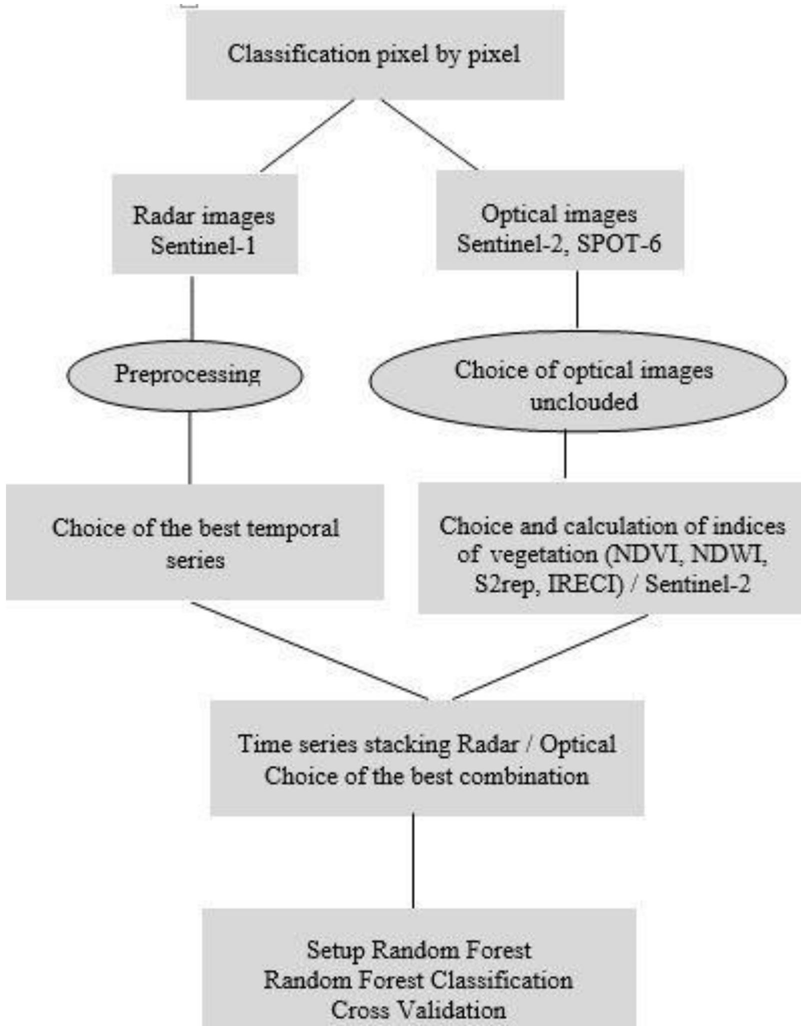


**In a first step**, the radar images Sentinel 1A images (Level 1 product) have been pre-processing: Multilook - Speckle filter - terrain Correction - Subset - Calibration. The treatment Multilook has for usefulness of a hand to reduce the noise inherent to an image with the combination of several images, and on the other hand to produce a product with a pixel size of nominal image. The multilooking is generated by the average of the cells and/or using the resolution azimuthal, thus increasing the radiometric resolution, but in degrading the spatial resolution. The "Speckle" (speckle noise level) is produced by interference which produce a "salt and pepper" effect on the image. The speckle-filter used is Lee sigma proposed by Lee (Lee, 1983). The Terrain Correction corrects the geometric distortions of radar images and georeferencing the images in a given projection using a MNT (digital model of terrain). The calibration corrects the radiometry of a SAR image so that the values of pixels really represent the radar backscatter of the reflecting surface. The corrections applied during calibration are specific to the mission, so the software automatically determines what the product images of entry you have and what corrections must be applied according to the metadata of the product. The calibration is essential for the quantitative use of SAR data. With regard to the optical images Sentinel-2, preprocessing is much more reduced because the images on the site of the ESA are already pre-processed. Sentinel-2 imagery is currently made available as Level 1C products.



Downloaded From: https://www.spiedigitallibrary.org/conference-proceedings-of-spie on 10/15/2018
Terms of Use: https://www.spiedigitallibrary.org/terms-of-use

**The second step** in the processing images consists in the calculation of the different indicators from the Sentinel-2A reflectance image. Various indices are used for assessing vegetation and soil properties in satellite remote sensing applications. A vegetation index can be an indicator to describe the greenness, density and health of vegetation. Four vegetation indices were calculated for the Sentinel-2A reflectance image: NDVI (*Normalized Difference Vegetation Index*, Rouse, Haas, Schell, Deering, & Harlan, 1974), NDWI (*Normalized Difference Water Index*, Gao, 1996), S2REP (*Sentinel-2 Red-Edge Position*, Frampton, Dash, Watmough, & Milton, 2013) et IRECI (*Inverted Red-Edge Chlorophyll Index*, Frampton, Dash, Watmough, & Milton, 2013).

NDVI is a commonly used vegetation index in remote sensing. This index is defined by the reflectance of red (RED) band and near infrared (NIR) band since they sense very different depths through vegetation canopies. RED channel locates in the strong chlorophyll absorption region while NIR channel has high vegetation canopy reflectance in this area.

$$\mathrm{NDVI} = \frac{\mathrm{NIR}-\mathrm{RED}}{\mathrm{NIR}+\mathrm{RED}} = \frac{\mathrm{B8}-\mathrm{B4}}{\mathrm{B8}+\mathrm{B4}} \quad \textbf{(1)}$$

NDWI was proposed by Gao (1996) to assess water status by the combination of NIR and short wave infrared (SWIR) channel because both are located in the high reflectance plateau of vegetation canopies and sense similar depth in vegetation canopies. Absorption by vegetation liquid water near NIR is negligible, and weak liquid absorption near SWIR is present. Therefore, canopy scattering enhances the water performance.

$$\mathrm{NDWI} = \frac{\mathrm{NIR}-\mathrm{SWIR}}{\mathrm{NIR}+\mathrm{SWIR}} = \frac{\mathrm{B8}-\mathrm{B12}}{\mathrm{B8}+\mathrm{B12}} \quad \textbf{(2)}$$

The S2REP red-edge index is based on linear interpolation (following the method of Guyot & Baret, 1988) by exploiting Sentinel-2A bands 5 and 6, both positioned on the red edge slope, at 705 and 740 nm respectively.

$$\mathrm{S2REP} = 705 + 35 * \frac{\frac{\mathrm{NIR}+\mathrm{RED}}{2}-\mathrm{RE1}}{\mathrm{RE2}-\mathrm{RE1}} = 705 + 35 * \frac{\frac{\mathrm{B8}+\mathrm{B4}}{2}-\mathrm{B5}}{\mathrm{B6}-\mathrm{B5}} \quad \textbf{(3)}$$

The inverted red-edge chlorophyll index (IRECI) which incorporates the reflectance in four S-2 bands to estimate canopy chlorophyll content. IRECI makes use of both RE bands, that S-2 will provide, to characterize the RE slope by using the reflectance at 740 nm and 705 nm while also making use of the maximum and minimum vegetation reflectance found in the NIR and red at 783 nm and 665 nm respectively (Frampton, Dash, Watmough, & Milton, 2013).

$$\mathrm{IRECI} = \frac{\mathrm{NIR}-\mathrm{RED}}{\frac{\mathrm{RE1}}{\mathrm{RE2}}} = \frac{\mathrm{B8}-\mathrm{B4}}{\frac{\mathrm{B5}}{\mathrm{B6}}} \quad \textbf{(4)}$$

**The third methodological step** is represented by time series stacking. After layer normalization to same value range, layer stacking was performed by adding all the processed radar and optical image layers.
The vegetation classification problem can be solved by using supervised learning algorithms. Supervised classification builds the implicit relationship between feature vector and target variable (i.e. class label) by learning from limited labelled training data (Russel et al., 1995). With the trained classification model, prediction can be made on new feature data such that its class label can be determined. To avoid overfitting the labelled data is usually divided into training set and testing set. Different classification algorithms have been developed in the literature including decision trees, discriminant analysis, Support Vector Machines (SVMs), nearest neighbor, neural network, etc. In this paper, Random Forest is chosen as the classifier algorithm assigning the same weight to each layer of the 44-bands layer stack image. The Random Forest (RF) approach applies a set of decision trees to improve prediction accuracy (Breiman, 2001). Decision trees are used more frequently in classification than in regression applications. Only lately the random forests approach gains popularity in applications with mapping of a diverse range of vegetation attributes e.g., biomass (Le Maire et al., 2011; Mutanga et al., 2012; Adam et al., 2014; Vaglio Laurin et al., 2014), canopy cover (Coulston et al., 2012; Gessner et al., 2013; Niculescu et al., 2018), LAI (Vuolo et al., 2014) and canopy nitrogen (Li et al., 2014). These studies typically demonstrate the higher



Downloaded From: https://www.spiedigitallibrary.org/conference-proceedings-of-spie on 10/15/2018
Terms of Use: https://www.spiedigitallibrary.org/terms-of-use

efficiency of the random forests method compared with the more conventional parametric and linear non-parametric methods (Verrelst et *al*., 2015).
In this study, the setting used for Random Forest was: Maximum depth of the tree (25), Minimum number of sample in each node (25) and Cluster possible values of a categorical variable into k (k=8).

SPOT images-6 have been classified by Random Forest and in combination with Sentinel-1.
Data pre-processing was performed with ESA Sentinel Application Platform toolbox (SNAP) for the Sentinel-1A data, and ESA SEN2COR processor for the Sentinel-2A imagery.
After layer normalization to same value range, layer stacking was performed by adding all the processed radar and optical image layers. The following image layers were stacked into a 44-layers image: Sentinel-1A VH and VV amplitude images (24); Sentinel-2A reflectance bands (13*10 + 24 = 154 bands); Sentinel-2A NDVI, S2REP, NDWI (44 bands), (Figure 4).

Figure 4: Processing chain of Time series stacking

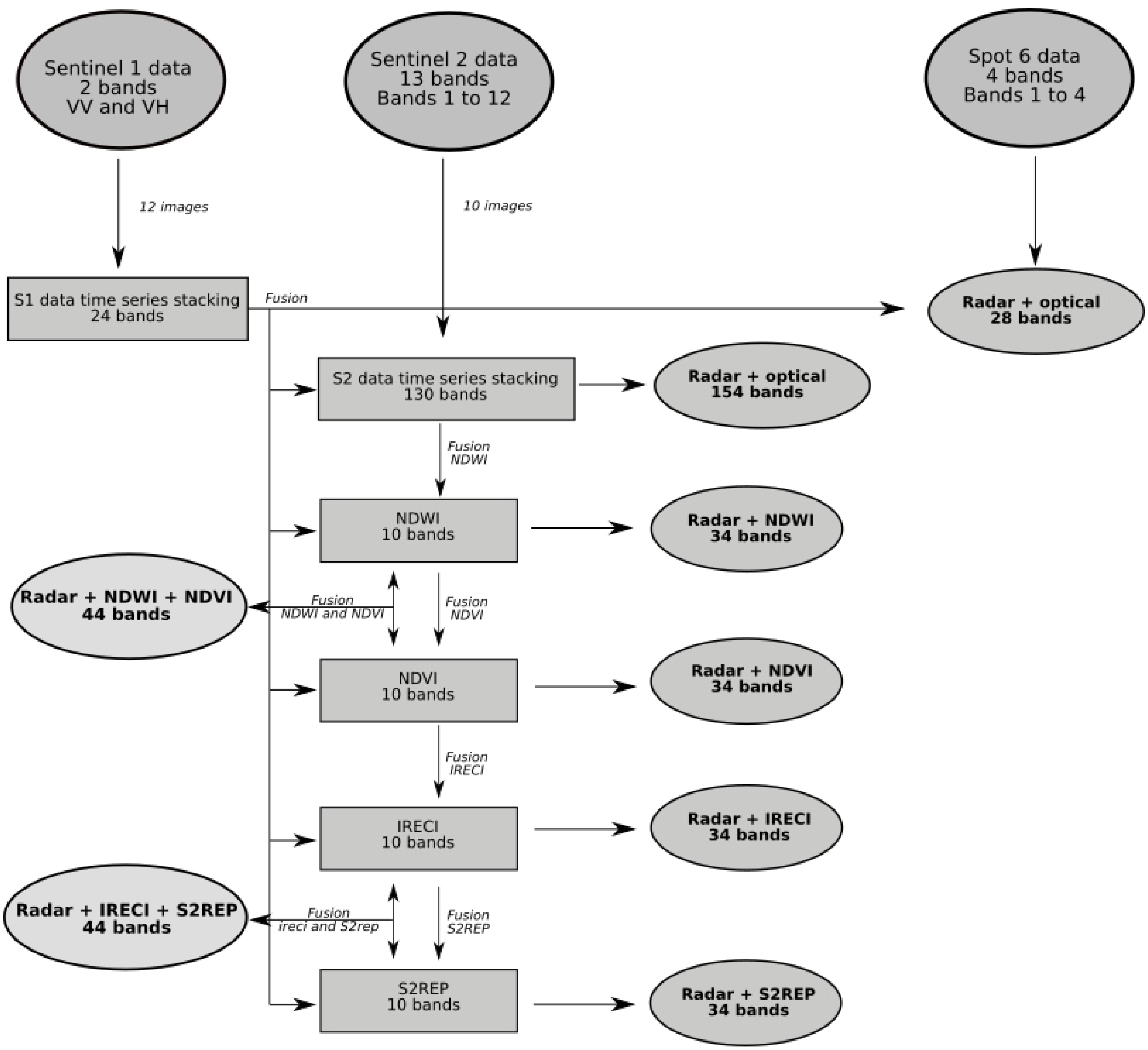




Downloaded From: https://www.spiedigitallibrary.org/conference-proceedings-of-spie on 10/15/2018
Terms of Use: https://www.spiedigitallibrary.org/terms-of-use

## 5- Results and Discussions

The objective of this study was to evaluate the performance of Random Forest method when applied to vegetation mapping from Sentinel-1, Sentinel-2 time-series data and SPOT-6. This algorithm are used to improve the accuracy of recognition and mapping of major vegetation classes in the Pays de Brest (France). A set of vegetation classes of interest were defined, namely: summer crops, winter crops, forest/ undergrowth, water, grassland, moors/lawns, no vegetation and sand dunes (Figure 5). These classes have been selected on the basis of the old classifications in the territory (Cesbios in 2016, Talab-Ou-Ali et *al*., 2017), observation conducted on the territory (photo-interpretation), and various study of the vegetation (sheet habitat of the Crozon peninsula, Conservatoire National Botanique, Brest). These classes must be detectable on the images Sentinel (resolution of 10m). The selected classes relate to the major types of vegetation of Pays de Brest (France). The selection of samples is based on the crossing of the existing data, the classification carried out by CESBIO in 2016, the parcel register Chart 2016, the BD_2016 vegetation, with previous samples used in the study of (Talab-Ou-Ali et *al*., 2017), and finally by photo-interpretation (Spot 6, Google Map, Sentinel 2).

Figure 5: Vegetation classes

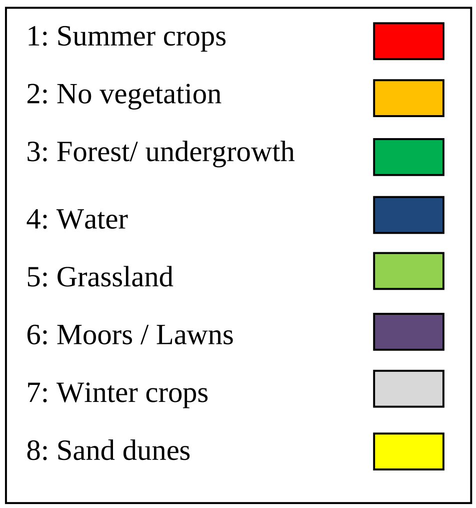


The results show very good classification performance for all combinations. The mapping accuracies were summarized producer and overall accuracy and Cohen's K (table 6, 7 and 8 for the Sentinel data and table 10 for the SPOT-6 data).

Table 6: Overall accuracy and kappa index by class for the Random Forests classifications of the Zone 1

| Land cover classes | Accuracy (%) SAR+NDVI+NWDI | Accuracy (%) SAR + S2rep + IRECI | Accuracy (%) SAR + Optical |
|---|---|---|---|
| **Summer crops** | 84 | 74 | 75 |
| **No vegetation** | 95 | 92 | 98 |
| **Forest/ undergrowth** | 81 | 85 | 84 |
| **Water** | 100 | 100 | 100 |
| **Grassland** | 83 | 87 | 73 |
| **Moors / Lawns** | 61 | 66 | 71 |
| **Winter crops** | 77 | 71 | 61 |
| **Sand dunes** | - | - | - |
| **Kappa index** | **0.91** | **0.89** | **0.91** |



Downloaded From: https://www.spiedigitallibrary.org/conference-proceedings-of-spie on 10/15/2018
Terms of Use: https://www.spiedigitallibrary.org/terms-of-use

| | | | |
|---|---|---|---|
| **OA** | **0.96** | **0.95** | **0.96** |

Table 7: Overall accuracy and kappa index by class for the Random Forests classifications of the Zone 2

| Land cover classes | Accuracy (%) SAR+NDVI+NWDI | Accuracy (%) SAR + S2rep + IRECI | Accuracy (%) SAR + Optical |
|---|---|---|---|
| **Summer crops** | 72 | 77 | 71 |
| **No vegetation** | 87 | 87 | 86 |
| **Forest/ undergrowth** | 85 | 88 | 88 |
| **Water** | 100 | 100 | 100 |
| **Grassland** | 89 | 91 | 89 |
| **Moors / Lawns** | 83 | 87 | 84 |
| **Winter crops** | 75 | 77 | 71 |
| **Sand dunes** | 97 | 96 | 97 |
| **Kappa index** | **0.91** | **0.92** | **0.91** |
| **OA** | **0.96** | **0.97** | **0.96** |

Table 8: Overall accuracy and kappa index by class for the Random Forests classifications of the Zone 5

| Land cover classes | Accuracy (%) SAR+NDVI+NWDI | Accuracy (%) SAR + S2rep + IRECI | Accuracy (%) SAR + Optical |
|---|---|---|---|
| **Summer crops** | 81 | 76 | 71 |
| **No vegetation** | 88 | 87 | 88 |
| **Forest/ undergrowth** | 91 | 92 | 93 |
| **Water** | 100 | 100 | 100 |
| **Grassland** | 89 | 83 | 74 |
| **Moors / Lawns** | 82 | 77 | 75 |
| **Winter crops** | 75 | 73 | 75 |
| **Sand dunes** | 74 | 97 | 97 |
| **Kappa index** | **0.91** | **0.91** | **0.89** |
| **OA** | **0.96** | **0.96** | **0.96** |

Following standard accuracy calculation procedures (Congalton & Green, 2008), we estimated an overall accuracy of 96-97%, and a Kappa Global coefficient between of 0.89 and 0.92. A detailed confusion matrix of the integrated datasets Random Forest-classified map, with overall, user and producer class accuracies, is reported in Table 9 (for the classification SAR + S2rep + IRECI).

Table 9: Confusion matrix and classification accuracy measures of the integrated datasets Random Forest-classified map of Zone 5 (SAR + S2rep + IRECI)

| Classification | Summer crops | No veget | Forest/ undergrowth | Wate r | Gras sland | Moors /Lawns | Winter crops | Sand dune | Accuracy (%) |
|---|---|---|---|---|---|---|---|---|---|
| **Summer crops** | 4040 | 8 | 16 | 0 | 265 | 13 | 399 | 0 | 77 |



Downloaded From: https://www.spiedigitallibrary.org/conference-proceedings-of-spie on 10/15/2018
Terms of Use: https://www.spiedigitallibrary.org/terms-of-use

| | | | | | | | | | |
|---|---|---|---|---|---|---|---|---|---|
| **No veget** | 0 | 1974 | 33 | 0 | 5 | 89 | 0 | 99 | 87 |
| **Forest/ undergrowth** | 0 | 0 | 3519 | 0 | 64 | 366 | 0 | 0 | 88 |
| **Water** | 0 | 0 | 0 | 121277 | 14 | 0 | 0 | 0 | 100 |
| **Grassland** | 122 | 10 | 11 | 0 | 5989 | 20 | 101 | 0 | 91 |
| **Moors /Lawns** | 0 | 0 | 217 | 0 | 585 | 5158 | 0 | 0 | 87 |
| **Winter crops** | 1554 | 0 | 0 | 0 | 131 | 0 | 3666 | 0 | 77 |
| **Sand dunes** | 0 | 169 | 0 | 0 | 0 | 0 | 0 | 3821 | 96 |
| | | | | | | | **Overall Accuracy kappa** | | 92 |

Table 10: Overall accuracy and kappa index by class for the Random Forests classifications of the Zone 5 of SPOT-6 images

| Land cover classes | Accuracy (%) Optical SPOT-6 | Accuracy (%) Optical SPOT-6 + Radar Sentinel-1 |
|---|---|---|
| **Summer crops** | 37 | 76 |
| **No vegetation** | 46 | 69 |
| **Forest/ undergrowth** | 66 | 80 |
| **Water** | 100 | 100 |
| **Grassland** | 62 | 88 |
| **Moors / Lawns** | 69 | 77 |
| **Winter crops** | 52 | 73 |
| **Sand dunes** | 60 | 93 |
| **Kappa index** | **0.75** | **0.89** |
| **OA** | **0.91** | **0.96** |

With the combination of multi-temporal radar Sentinel-1 and the vegetation indices NDVI, and NWDI that crops are the best detected and classified primarily in the Zone 1 and 2 (more than 80% accuracy), and to a lesser extent with the combination optical/radar. The distinction between crops/grassland is complex because these vegetation have similarities spectral and texture. In the area 5 (Crozon Peninsula), the combination multi-temporal radar and the vegetation indices S2rep and IRECI presents the accuracy of the more important (77%) whereas in the other combinations, for this zone, it remains around 71-72%. The major confusion of this class is indeed the class grassland. Images acquired on seven consecutive years are necessary to distinguish between them, the cultures and the Prairies being regarded as temporary when they are returned at least once on this period (Lecerf, 2008).

The results concerning forests/ undergrowth are almost similar from one classification to the other. The forests are very well identified with the three categories of combinations, but are however much better classified on the classifications obtained from the combination radar/optical for zone 1 (93% accuracy), to the detriment of undergrowth . The results from the processing of combinations of the radar with the various indices of vegetation are also good for all three zones (details above 80%). The herbaceous vegetation (grassland), are fairly well identified and classified irrespective of the combination used. We mention that the radar combinations/optics are less favorable to the identification of this class.

The class Moors / lawns presents a good classification in particular on the Zone 5, area where this class is well represented. The combinations of the radar image with the various indices of vegetation are very favorable to the identification of this



Downloaded From: https://www.spiedigitallibrary.org/conference-proceedings-of-spie on 10/15/2018
Terms of Use: https://www.spiedigitallibrary.org/terms-of-use

class. The results less good have been registered for the Zone 2 with accuracy, slightly higher than 60%. This class in Zone 2 is under-represented from a space point of view.

There are some differences between the three classifications of Zone 5. Firstly there is inconsistency of classifications with the classes non-vegetation and dunes/sands and between forest/ undergrowth and moors/lawn. These inconsistencies are observed with the classification using indices S2rep/IRECI. With these indices, areas of non-vegetation (cliffs, roads) sometimes find themselves classified in the class dune/sand as shown in the Figure 4. Similarly, although this is rarer, of clearly defined zones as Moors (Figure 6 and Figure 7) find themselves classified forest/undergrowth. The use of the NDVI indices/NDWI joined the classification using the optical data and complete radars with less errors of classifications.

Figure 6: Error of classifications between the classes Non-vegetation and sand/dune

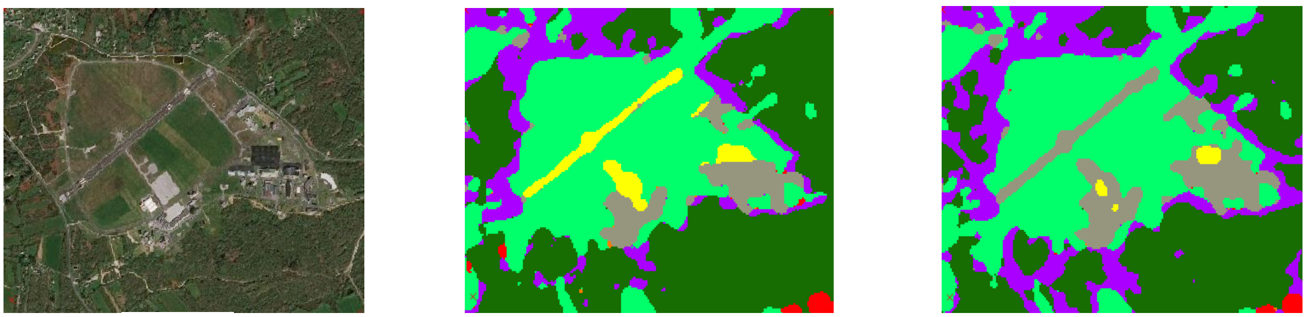

Spot 6 S2REP + IRECI +radars NDVI + NDWI +radars

Figure 7: Error of classifications between the classes forest/undergrowth and moors/lawn

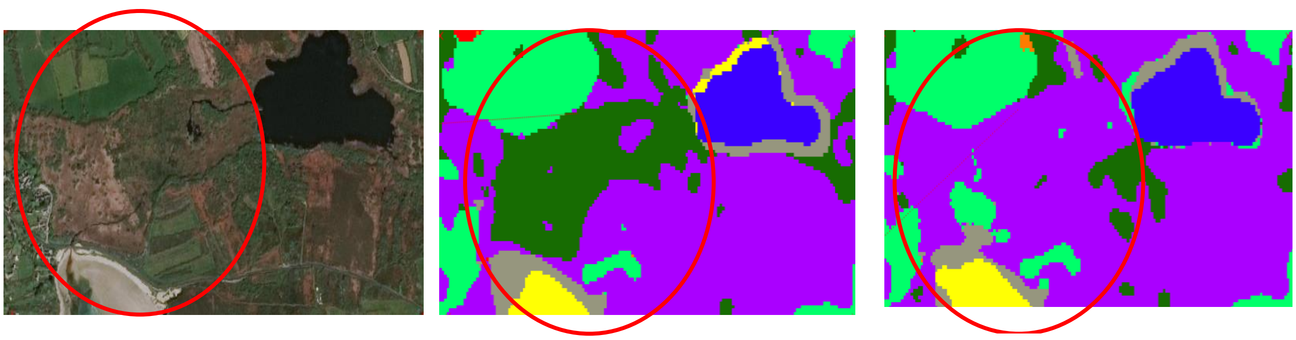

Spot 6 S2REP + IRECI +radars NDVI + NDWI +radars

The use of the index NDVI NDWI/therefore seems to be more effective for the classification of major types of vegetation for Pays de Brest, proposing a classification rather uniform and consistent. Nevertheless the use of indices S2REP and IRECI could be more useful to differentiate the classes "close", as for the differentiation of association of vegetation.

The comparison of the Kappa coefficients Global on the three sites shows that the three combinations, in a general way, have conclusive results for the identification, monitoring and mapping of the vegetation of the area studied. In in the second time, it is interesting to follow the accuracy of the mapping by class. This precision of map varies as a function of the sensitivity of these combinations to the textural characteristics, structural, space of the different classes of vegetation (Figure 8 and Figure 9).



Downloaded From: https://www.spiedigitallibrary.org/conference-proceedings-of-spie on 10/15/2018
Terms of Use: https://www.spiedigitallibrary.org/terms-of-use

Figure 8: Random Forest Classification by Time series stacking of Sentinel-1 and Sentinel-2 images

| Time series stacking: SAR + NDVI + NDWI | Time series stacking: SAR + S2rep + IRECI | Time series stacking: SAR + Optical |
|---|---|---|
| 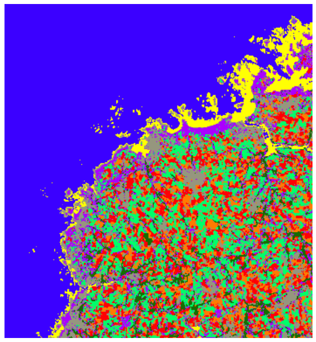 ZONE 1 | 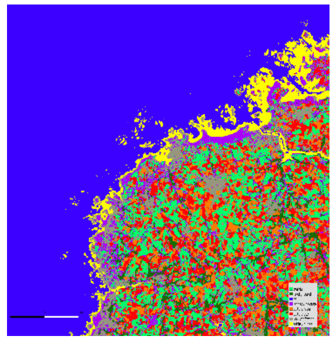 ZONE 1 | 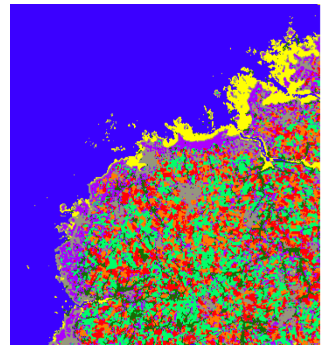 ZONE 1 |
| 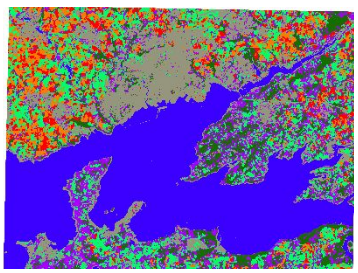 ZONE 2 | 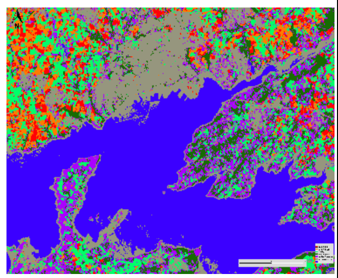 ZONE 2 | 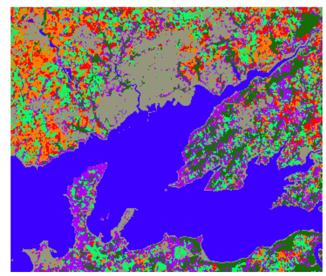 ZONE 2 |
| 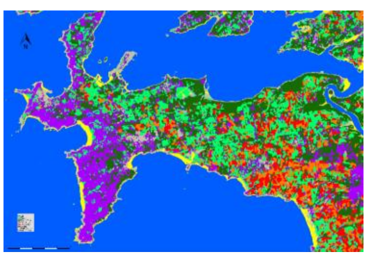 ZONE 5 | 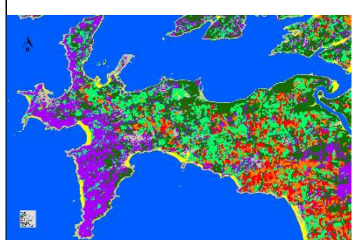 ZONE 5 | 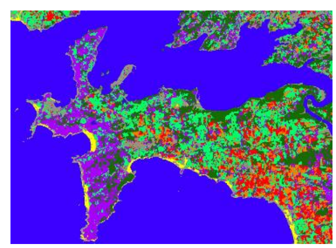 ZONE 5 |

Figure 9: Random Forest Classification by Time series stacking of SPOT-6 and Sentinel-1 images of Zone 5

| | |
|---|---|
| 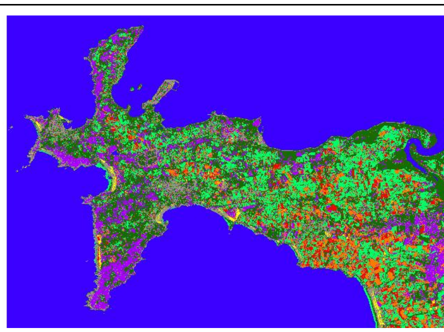 Stacking of SPOT-6 | 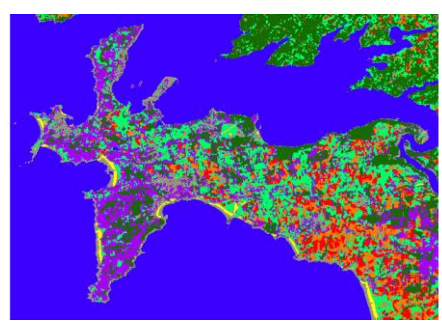 Time series stacking of SPOT-6 and Sentinel-1 |



Downloaded From: https://www.spiedigitallibrary.org/conference-proceedings-of-spie on 10/15/2018
Terms of Use: https://www.spiedigitallibrary.org/terms-of-use

The results of processing of the SPOT-6 image show results less good in comparisons with the results of classification of the series multi-temporal Sentinel-1 especially for the classes as summer crops (37%) or winter crops (52%). The multi-temporalities of radar data Sentinel-1 is required with more accuracy and clarity in the results of the classifications.

## 6- Conclusion

This study has permitted to produce a new processing chain reproducible by time series stacking with Sentinel-1, Sentinel-2 and SPOT-6 using machine learning techniques (Random Forest), to identify and to monitoring the vegetation at a single level typological - the major types of vegetation of the Pays de Brest. In general, the results from the processing of images Sentinel-1 and Sentinel-2 are promising (Kappa coefficient between 0.89 and 0.91 depending on the level of validation) as well as those derived from the processing of SPOT images-6 (Kappa coefficient between and depending on the level of validation). The images Sentinel-1 and Sentinel-2 provides a great opportunity for global vegetation monitoring due to its enhanced spatial, spectral and temporal characteristics compared with SPOT. The methods are only based on a few input parameters and provide accurate classification results. Increasing the number of images improves the accuracy of the classifications of the vegetation.

Three combinations classification methods are studied and compared, namely index-based classification (NDVI, NDWI) with SAR data, index-based classification (S2rep and IRECI) with SAR data and SAR data with optical images. The inclusion of vegetation indices added important information for the discrimination between forests, crops and grassland. The presence of red edge bands in the Sentinel-2 MSI imagery represents a significant spectral enrichment with respect to other commonly used sensors in vegetation mapping. In addition, the methodology Time Series stacking improves the results clearly notably at the level of the processing of images of the entire year, a very important aspect for the identification and mapping of the vegetation. The algorithm Random Forest classifier is less sensitive than other streamline machine learning classifiers to the quality of training samples and to overfitting, due to the large number of decision trees produced by randomly selecting a subset of training samples and a subset of variables for splitting at each tree node.

The study indicates satisfactory results and suggests good potential for mapping the vegetation in the study area. The free and open-source Sentinel imagery in both SAR and multispectral data and the associated open-source SNAP software and Orfeo Tool Box should encourage the conduct of vegetation mapping and monitoring in the coastal zone.

The classification procedures produced from the 23 images are reproducible which allows their implementation on vast territories. The maps produced are of interest to highlight ecological continuity between sectors to issues for biodiversity.

### Acknowledgements

This work was supported by the CNES (Centre National d’Etudes Spatiales).

## REFERENCES

[1] Adam E., Mutanga O., Odindi J. & Abdel-Rahman E., M. (2014). Land-use/cover classification in a heterogeneous coastal landscape using RapidEye imagery: evaluating the performance of random forest and support vector machines classifiers, International Journal of Remote Sensing, 35:10, 3440-3458.

[2] Bargiel, D., (2017). A new method for crop classification combining time series of radar images and crop phenology information. Remote Sensing of Environment 198, 369–383.

[3] Barrett, B., Raab, C., Cawkwell, F., Green, S., (2016). Upland vegetation mapping using Random Forests with optical and radar satellite data. Remote Sensing in Ecology and Conservation 2, 212–231.



Downloaded From: https://www.spiedigitallibrary.org/conference-proceedings-of-spie on 10/15/2018
Terms of Use: https://www.spiedigitallibrary.org/terms-of-use

[4] Belgiu, M., Drăguţ, L., (2016). Random forest in remote sensing: A review of applications and future directions. ISPRS Journal of Photogrammetry and Remote Sensing 114, 24–31.

[5] Breiman, L., (2001). Random Forests. Machine Learning 45, 5–32.

[6] Chappelle, E.W., Kim, M.S. and McMurtrey, J.E. (1992). Ratio analysis of reflectance spectra (RARS): an algorithm for the remote estimation of the concentrations of chlorophyll a, chlorophyll b, and carotenoids in soybean leaves. Remote Sensing Environment, 39: 239-247.

[7] Chilar, J., (2000), Land cover mapping of large areas from satellites: Status and research priorities. International Journal of Remote Sensing, 21(6), 1093–1114.

[8] Congalton, R.G., Green, K., (2008). Assessing the accuracy of remotely sensed data: principles and practices. CRC press.

[9] Coulston, J.W., Moisen, G.G., Wilson, B.T., Finco, M.V., Cohen, W.B., Brewer, C.K., (2012). Modeling percent tree canopy cover: a pilot study. Photogrammetric Engineering & Remote Sensing 78(7): 715–727 78, 715–727.

[10] Du, P., Samat, A., Waske, B., Liu, S., Li, Z., (2015). Random Forest and Rotation Forest for fully polarized SAR image classification using polarimetric and spatial features. ISPRS Journal of Photogrammetry and Remote Sensing 105, 38–53.

[11] Esch, T., Metz, A., Marconcini, M., Keil, M., (2014). Combined use of multi-seasonal high and medium resolution satellite imagery for parcel-related mapping of cropland and grassland. International Journal of Applied Earth Observation and Geoinformation 28, 230–237.

[12] Forkuor, G.; Conrad, C.; Thiel, M.; Ullmann, T.; Zoungrana, E. (2014). Integration of Optical and Synthetic Aperture Radar Imagery for Improving Crop Mapping in Northwestern Benin, West Africa. Remote Sensing, *6*, 6472-6499.

[13] Frampton, W.J., Dash, J., Watmough, G., Milton, E.J., (2013). Evaluating the capabilities of Sentinel-2 for quantitative estimation of biophysical variables in vegetation. ISPRS Journal of Photogrammetry and Remote Sensing 82, 83–92.

[14] Gao, B., (1996). NDWI—A normalized difference water index for remote sensing of vegetation liquid water from space. Remote Sensing of Environment 58, 257–266.

[15] Gessner, U., Machwitz, M., Conrad, C., Dech, S., (2013). Estimating the fractional cover of growth forms and bare surface in savannas. A multi-resolution approach based on regression tree ensembles. Remote Sensing of Environment 129, 90–102.

[16] Guyot, G. & Baret, F., Utilisation de la Haute Résolution Spectrale pour Suivre L'état des Couverts Végétaux, Spectral Signatures of Objects in Remote Sensing, Proceedings of the conference held 18-22 January, (1988) in Aussois (Modane), France. Edited by T.D. Guyenne and J.J. Hunt. ESA SP-287. European Space Agency, p.279.

[17] Hong, S.-H., Kim, H.-O., Wdowinski, S., Feliciano, E., (2015). Evaluation of Polarimetric SAR Decomposition for Classifying Wetland Vegetation Types. Remote Sensing 7, 8563–8585.

[18] Hill M. J., Ticehurst C. J., Lee Jong-Sen, Grunes M. R., Donald G. E. and Henry D., (2005). Integration of optical and radar classifications for mapping pasture type in Western Australia, in IEEE Transactions on Geoscience and Remote Sensing, vol. 43, no. 7, pp. 1665-1681.

[19] Huete, A. R., Liu, H. Q., Batchily, K., & van Leeuwen,W., (1997). A comparison of vegetation indices over a global set of TM images for EOS-MODIS. *Remote Sensing of Environment*, *59*, 440−451.

[20] Huete, A., Justice, C., & Liu, H., (1994). Development of vegetation and soil indices for MODIS-EOS. *Remote Sensing of Environment*, *49*, 224−234.



Downloaded From: https://www.spiedigitallibrary.org/conference-proceedings-of-spie on 10/15/2018
Terms of Use: https://www.spiedigitallibrary.org/terms-of-use

[21] Kuemmerle, T., Erb, K., Meyfroidt, P., Müller, D., Verburg, P. H., Estel, S., Reenberg, A. (2013). Challenges and opportunities in mapping land use intensity globally. Current Opinion in Environmental Sustainability, 5(5), 484–493.

[22] Laurin, G.V., Chan, J.C.-W., Chen, Q., Lindsell, J.A., Coomes, D.A., Guerriero, L., Frate, F.D., Miglietta, F., Valentini, R., (2014). Biodiversity Mapping in a Tropical West African Forest with Airborne Hyperspectral Data. PLOS ONE 9, e97910.

[23] Le Maire, G., Marsden, C., Nouvellon, Y., Grinand, C., Hakamada, R., Stape, J.-L., Laclau, J.-P., (2011). MODIS NDVI time-series allow the monitoring of Eucalyptus plantation biomass. Remote Sensing of Environment 115, 2613–2625.

[24] Lecerf R., (2008). Suivi des changements d'occupation et d'utilisation des sols d'origine anthropique et climatique à l'échelle régionale par télédétection moyenne résolution (application à la Bretagne). Thèse de doctorat. Université de Rennes 2, Rennes, 326 p.

[25] Li, H., Leung, K.-S., Wong, M.-H., Ballester, P.J., (2014). Substituting random forest for multiple linear regression improves binding affinity prediction of scoring functions: Cyscore as a case study. BMC Bioinformatics 15, 291.

[26] Montesano, P.M., Cook, B.D., Sun, G., Simard, M., Nelson, R.F., Ranson, K.J., Zhang, Z., Luthcke, S., (2013). Achieving accuracy requirements for forest biomass mapping: A spaceborne data fusion method for estimating forest biomass and LiDAR sampling error. Remote Sensing of Environment 130, 153–170.

[27] Mulla, D. J. (2013). Twenty five years of remote sensing in precision agriculture: Key advances and remaining knowledge gaps. *Biosystems Engineering*, *114*(4), 358–371.

[28] Mutanga, O., Adam, E., Cho, M.A., (2012). High density biomass estimation for wetland vegetation using WorldView-2 imagery and random forest regression algorithm. International Journal of Applied Earth Observation and Geoinformation 18, 399–406.

[29] Niculescu S., Lardeux C., Grigoras I., Hanganu J., et David L., (2016). Synergy Between LiDAR, RADARSAT-2, and Spot-5 Images for the Detection and Mapping of Wetland Vegetation in the Danube Delta », IEEE Journal of Selected Topics in Applied Earth Observations and Remote Sensing, vol. 9, nº 8, p. 3651‑3666.

[30] Niculescu S., Lardeux C., Hanganu J., (2017). Alteration and Remediation of Coastal Wetland Ecosystems in the Danube Delta. A Remote-Sensing Approach. Springer International Publishing. Alteration and Remediation of Coastal Wetland Ecosystems, vol. 21 (17), Springer International Publishing, pp.513-554, 2017, Coastal Research Library.

[31] Peters J., Coillie F. V., Westra T. & Wulf Robert De (2011). Synergy of very high resolution optical and radar data for object-based olive grove mapping, International Journal of Geographical Information Science, 25:6, 971-989.

[32] Reiche, J., ( 2015). Combining SAR and optical satellite image time series for tropical forest monitoring.

[33] Rodrigues, S.W.P., Souza-Filho, P.W.M., (2011). Use of Multi-Sensor Data to Identify and Map Tropical Coastal Wetlandsin the Amazon of Northern Brazil. Wetlands 31, 11–23.

[34] Rodriguez-Galiano, V.F., Ghimire, B., Rogan, J., Chica-Olmo, M., Rigol-Sanchez, J.P., (2012). An assessment of the effectiveness of a random forest classifier for land-cover classification. ISPRS Journal of Photogrammetry and Remote Sensing 67, 93–104.

[35] Rouse J.W., Haas R.H., Schell J.A., Deering D.W. & J.C. Harlan, (1974). Monitoring the Vernal Advancement and Retrogradation (Green Wave Effect) of Natural Vegetation, *NASA/GSFC Type III Final Report, Greenbelt, MD., 371p.*



Downloaded From: https://www.spiedigitallibrary.org/conference-proceedings-of-spie on 10/15/2018
Terms of Use: https://www.spiedigitallibrary.org/terms-of-use

[36] Schuster, C., Schmidt, T., Conrad, C., Kleinschmit, B., Förster, M., (2015). Grassland habitat mapping by intra-annual time series analysis – Comparison of RapidEye and TerraSAR-X satellite data. International Journal of Applied Earth Observation and Geoinformation 34, 25–34.

[37] Talab Ou Ali H., Niculescu S., Sellin V., Bougault C., (2017). Contribution of the new satellites (Sentinel-1, Sentinel-2 and SPOT-6) to the Coastal Vegetation Monitoring in the Pays de Brest (France). SPIE DIGITAL LIBRARY, Remote Sensing for Agriculture, Ecosystems, and Hydrology XIX, 10421 (1042129), 17 p.

[38] Torres, R., Snoeij, P., Geudtner, D., Bibby, D., Davidson, M., Attema, E., Rostan, F. (2012). GMES Sentinel-1 mission. Remote Sensing of Environment, 120, 9–24.

[39] Ullmann, T.; Schmitt, A.; Roth, A.; Duffe, J.; Dech, S.; Hubberten, H.-W.; Baumhauer, R. Land Cover Characterization and Classification of Arctic Tundra Environments by Means of Polarized Synthetic Aperture X- and C-Band Radar (PolSAR) and Landsat 8 Multispectral Imagery — Richards Island, Canada, (2014). Remote Sensing. 2014, *6*, 8565-8593.

[40] Verrelst, J., Rivera, J.P., Veroustraete, F., Muñoz-Marí, J., Clevers, J.G.P.W., Camps-Valls, G., Moreno, J., (2015). Experimental Sentinel-2 LAI estimation using parametric, non-parametric and physical retrieval methods – A comparison. ISPRS Journal of Photogrammetry and Remote Sensing 108, 260–272.

[41] Vuolo, F., Atzberger, C., (2014). Improving Land Cover Maps in Areas of Disagreement of Existing Products using NDVI Time Series of MODIS – Example for EuropeVerbesserung von Landbedeckungskarten in Gebieten widersprüchlicher Grundlagen mit Hilfe der NDVI-Zeitreihe von MODIS – Beispiel für Europa. Photogrammetrie - Fernerkundung - Geoinformation, 393–407.



Downloaded From: https://www.spiedigitallibrary.org/conference-proceedings-of-spie on 10/15/2018
Terms of Use: https://www.spiedigitallibrary.org/terms-of-use